Pakistan Veterinary Journal

ISSN: 0253-8318 (PRINT), 2074-7764 (ONLINE)
DOI: 10.29261/pakvetj/2026.056

RESEARCH ARTICLE

Combination of Acupoint-Targeted Subhypnotic Dexmedetomidine and Electroacupuncture as a Novel Multimodal Therapy for Alleviating Inflammatory Pain in Mice

Mahmoud M Abouelfetouh[1,2], Eman Salah[3], Hao Li[1], Meng Li[1], Amany Ramah[4,5], Muhammad Kashif Maan[1,6], Faisal Ayub Kiani[1,7], Mingxing Ding[1], Fei Huang[8*] and Yi Ding[1*]

[1]College of Veterinary Medicine, Huazhong Agricultural University, No.1, Shizishan Street, Hongshan District, Wuhan, Hubei Province, 430070, China; [2]Department of Surgery, Anesthesiology and Radiology, Faculty of Veterinary Medicine, Benha University, Moshtohor, 13736, Egypt; [3]Department of Pharmacology, Faculty of Veterinary Medicine, Benha University, Moshtohor, 13736, Egypt; [4]Laboratory of Veterinary Anatomy, Faculty of Agriculture, University of Miyazaki, Miyazaki 889-2192, Japan; [5]Department of Forensic Medicine and Toxicology, Faculty of Veterinary Medicine, Benha University, Moshtohor, 13736, Egypt; [6]Department of Veterinary Surgery, Faculty of Veterinary Science, University of Veterinary and Animal Sciences, Lahore, Pakistan; [7]Department of Clinical Sciences, Faculty of Veterinary Sciences, Bahauddin Zakariyah University, Multan, Pakistan; [8]Wuhan National Laboratory for Optoelectronics, Huazhong University of Science and Technology, Wuhan 430074, China.
*Corresponding author: dingyi@mail.hzau.edu.cn (YD); dfeihuang@163.com (FH)

ARTICLE HISTORY (25-882)

Received: September 13, 2025
Revised: December 26, 2025
Accepted: January 06, 2026
Published online: January 10, 2026

Key words:
Acupoint-delivered dexmedetomidine
Electroacupuncture
Inflammatory markers
Pain
RNA sequencing

ABSTRACT

Quality of life is markedly influenced by inflammatory pain, with current therapeutic options frequently necessitating extended treatment periods and resulting in many undesirable side effects. In the present study, a Complete Freund's Adjuvant (CFA)-induced model was employed to examine the therapeutic potential of electroacupuncture (EA) in conjunction with subhypnotic doses of dexmedetomidine (DEX) administered at acupoints for managing inflammatory pain. The experimental design involved 36 healthy male C57BL/6 mice equally divided into six experimental treatments: saline (SAL), CFA, diclofenac sodium standard treatment (ST), DEX, EA and combined DEX-EA, with six mice in each group. Treatments commenced 48h following CFA administration, consisting of four treatment sessions at two-day intervals. Following each treatment session, nociceptive thresholds were evaluated. After the last session, paw tissue samples collected from affected paws were subjected to histopathological and immunohistochemical examination, and RNA seq was performed on spinal cord specimens. Results revealed that the DEX-EA therapy produced significantly higher nociceptive thresholds compared to the CFA, DEX monotherapy, and EA monotherapy ($P<0.05$). Additionally, inflammatory indices showed significant improvements with the DEX-EA, with decreased levels of CD45, MPO, TNF-α, IL-6, and IL-1β compared to the CFA, DEX monotherapy, and EA monotherapy ($P<0.05$). Compared to the CFA, non-significant variations were found in nociceptive thresholds and IL-6 level in the DEX and EA monotherapies; however, a significant decrease was found in the level of CD45, MPO, and IL-1β ($P<0.05$). Transcriptomic data revealed 65 differentially expressed genes (DEGs), demonstrating enhanced expression of genes associated with GABAergic neurotransmission, degradative pathways, and autophagic mechanisms. The findings demonstrate that combining EA with DEX produces synergistic anti-nociceptive and anti-inflammatory effects mediated through spinal cord mechanisms.

To Cite This Article: Abouelfetouh MM, Salah E, Li H, Li M, Ramah A, Maan MK, Kiani FA, Ding M, Fei H and Ding Y, 2026. Combination of acupoint-targeted subhypnotic dexmedetomidine and electroacupuncture as a novel multimodal therapy for alleviating inflammatory pain in mice. Pak Vet J, 46(3): 670-680. http://dx.doi.org/10.29261/pakvetj/2026.056

INTRODUCTION

One of the widespread health issues worldwide is pain that is mediated by inflammation. It affects millions of individuals and pushes medical services to the limit everywhere. The traditional pharmacological methods of managing inflammatory pains such as non-steroidal anti-inflammatory drugs (NSAIDs), corticosteroids, and opioids are conventional treatment modalities. Nevertheless, these drugs require prolonged administration and have high chances of adverse reactions. Subsequently, the creation of therapeutic options with proven efficacy and positive tolerability profiles is an urgent topic in the management of inflammatory pain syndromes (Lynch and Watson, 2006; Ho *et al.*, 2018).

Because acupuncture is combined with the use of low doses of therapeutic substances, it is an effective method known as pharmaco-puncture (Park *et al.*, 2023). This integrated program works well in the management of pains and the disorders associated with it. It focuses on pain modulation and some biological pathways associated with inflammation. Medications placed at the acupoints have a direct effect on local immune cells, blood vessels, and nerve endings, which stimulate better therapeutic effects using small amounts of systemic drugs and reducing side effects (Vieira *et al.,* 2018; Son *et al.,* 2024).

Electroacupuncture (EA), which is a modern form of manual acupuncture, i.e. the combination of manually inserted needles and electrically-induced stimulation of the needles at the particular acupoints, is often employed to treat the neurological, musculoskeletal, and pain-related disorders (Li *et al.,* 2018). Electroacupuncture could be used to decrease inflammation and pain through the stimulation of the expression of endogenous opioids and through the regulation of the release of inflammatory cytokines (Gondim *et al.,* 2012; Park and Namgung, 2018; Lan *et al.,* 2024). Moreover, EA has an opportunity of enhancing the effectiveness and multimodal synergistic effects of acupoint drug injections in pain relief.

Dexmedetomidine (DEX) is a selective α2-adrenergic receptor agonist, which is a sedative, analgesic and anti-inflammatory agent. It has been previously demonstrated that DEX has the ability to inhibit the nuclear factor-kappa beta (NF-κB) inflammatory pathways and inhibit the production of cytokines, further broadening its potential role in pain management (Li *et al.,* 2015; Ji *et al.,* 2017). Transmembrane glycoprotein (CD45) and myeloperoxidase (MPO) are regarded as key markers of inflammatory cellular infiltration linked with immune cell response, which is positively correlated with the level of the released cytokines (Oikonomou *et al.,* 2023). The spinal cord has a pivotal role in the management of inflammatory pain through regulating the expression of genes related to pain pathway, including the gamma aminobutyric acid type A receptor (Liu *et al.,* 2025) and chemokine-related genes (Cao *et al.*, 2014).

However, there is relatively little information available in the literature regarding the use of EA as an intervention together with DEX administered at acupoints to reduce inflammatory pain. Hence, this study was planned with the following objectives: 1) To investigate the antinociceptive and anti-inflammatory effects of DEX and EA given at particular acupoints in a Complete Freund's Adjuvant (CFA)-induced inflammatory pain model; and 2) To assess the RNA-seq of the spinal cord to reveal the potential underlying mechanisms and enriched functional pathways. The hypothesis was that EA and acupoint-administered DEX would be synergistic and would be more effective in pain relief and less inflammatory than either treatment. This multimodal strategy has the potential to provide an innovative and integrative method of dealing with inflammatory pain with reduced systemic side effects.

MATERIALS AND METHODS

Animals: The study used 36 healthy male C57BL/6 mice aged between 6-8 weeks and 18-22g to serve as the experimental units (licensing number SCXK (Hubei) 2020-0019). Animals were maintained under controlled conditions with ambient temperatures at 22±1°C, relative humidity between 50 and 60%, and alternating 12-hour periods of illumination and darkness, with unrestricted access to a standard mice diet and water. Following a seven-day adaptation period, the experimental units were tested for baseline mechanical and thermal threshold values before the start of the formal experiment. During the preliminary test, seven mice were excluded from subsequent experiments because they showed delayed or exaggerated responses and were replaced with animals displaying normal baseline responses.

Experimental design: Mice were randomly assigned (n=6/group) to: (1) SAL: given normal saline injection (25μL, plantar left hind-paw); (2) CFA: given 20μL CFA (1mg/mL *Mycobacterium tuberculosis*, H37Ra) (Yu *et al.,* 2021); (3) ST: given CFA+diclofenac sodium standard treatment (10mg/kg IP) (Gupta *et al.,* 2015); (4) DEX: given CFA+subhypnotic DEX (1.4μg/kg) at ST36; (5) EA: given CFA+EA at ST36; (6) DEX-EA: given CFA+DEX at ST36+EA. In this study, the ST36 denotes the acupuncture point stomach 36. Treatments began two days post-CFA and were repeated every two days for four treatment sessions. Pain thresholds were measured before CFA and after each treatment session (days 2, 4, 6, 8). After the last session, blood was collected for testing blood cortisol, and animals were then sacrificed for tissue collection. Paw tissue samples were preserved in 4% paraformaldehyde (PFA) for histology and immunohistochemistry, while L4–L6 spinal cords were snap-frozen for RNA-seq. Schematic representation of experimental procedures and therapeutic interventions implemented throughout the CFA inflammation study, depicting timepoints of treatments, evaluation points, and specimen collection is shown in Fig. 1A.

Acupoint-delivered DEX and EA: Before the start of the formal experiment (pretest period), several subhypnotic doses of DEX were injected at the ST36 acupoints, pain thresholds were tested, and the dose of DEX selected for this study was determined to conduct the formal test. A subhypnotic concentration of DEX (1.4μg/kg, TCI, Japan) diluted in 100μL saline solution (50μL per side) was administered bilaterally at the ST36 acupoint (positioned 4mm lateral from the tibial tubercle at 2-3mm insertion depth). Anatomical illustration depicting ST36 acupoint localization utilized for both EA stimulation and DEX

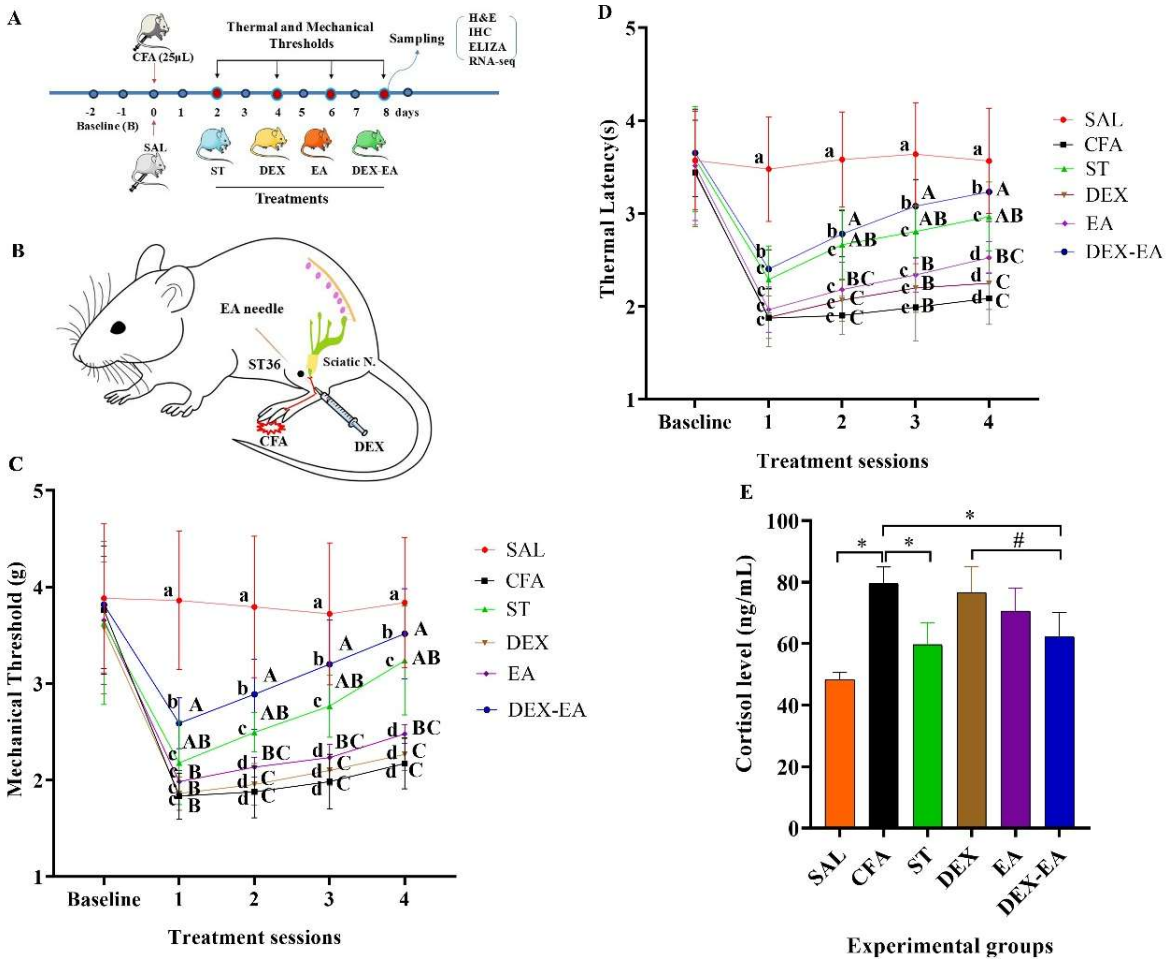

Fig. 1: A): Schematic representation of timepoints and experimental procedures. B): Anatomical illustration depicting ST36 acupoint localization. C): Mechanical nociceptive thresholds(g) across treatment cohorts. D): Thermal latency(s) among treatment cohorts. E): Cortisol concentrations (ng/mL) across experimental cohorts. Letters (a–d) denote statistically significant deviations from SAL controls (P<0.05); capital letters (A–C) represent significant inter-group variations (P<0.05). (*) signifies notable differences from CFA controls (P<0.05); (#) demonstrates significant between-group distinctions (P<0.05).

delivery is shown in Fig. 1B. Electroacupuncture procedures were conducted according to established protocols (Koo *et al.,* 2010; Wan *et al.,* 2020). After 3 days of being habituated on restraint equipment, stainless steel acupuncture needles with a diameter of 0.30mm and a length of 13mm were inserted at ST36 points, attached to a WQ-6F Acupunctoscope device and subjected to electrical stimulation with square wave pulses of 2.0Hz frequency and 133mA intensity, over a 30-minute period.

Nociceptive threshold measurement: Nociceptive threshold assessment was carried out in terms of mechanical sensitivity assessment and thermal sensitivity evaluation. For mechanical sensitivity assessment, paw withdrawal threshold (PWT) evaluation utilized an electronic Von Frey aesthesiometer equipped with a 0.5mm probe. Force application to the plantar region continued until a withdrawal response occurred; measurements from three consecutive trials were recorded for mean calculation. For thermal sensitivity evaluation, paw withdrawal latency (PWL) assessment employed a heated platform maintained at 55°C (maximum exposure duration 30s). The plate surfaces were cleaned between the individual assessments using 75% alcohol (Manglik *et al.,* 2016).

Serum cortisol: Blood samples (0.5–0.7mL) obtained via submandibular venipuncture underwent centrifugation (1,000–2,000×g for 10min). The obtained serum samples were stored at –20°C. Cortisol was quantified using ELISA (Shanghai Yuanju Biotechnology) following manufacturer's protocols. The cortisol assay sensitivity was less than 0.1ng/mL. Also, the intra-assay and inter-assay CVs were less than 15%. The assay optical density was measured at a 450nm wavelength. The standard curve was plotted in an Excel spreadsheet, and the concentration of each sample was calculated from the equation derived from the curve.

Histopathology: Paw width (PW) was measured with calipers. For microscopic examination, paw tissues were kept in 4% PFA, embedded in paraffin, sectioned at 5μm thickness, and stained with H&E (Suvarna *et al.,* 2013). Inflammation was scored at a scale of 0 to 5, as described earlier (Hussein *et al.*, 2013), and quantified by ImageJ, with infiltrating cells counted relative to SAL controls.

Immunohistochemistry: Paraffin-embedded paw slices (5μm) were treated with Tris-EDTA antigen retrieval (pH 9.0), H_2O_2 peroxidase blocking solution (3%), and serum blocking solution. Sections were incubated in the refrigerator

(4°C) overnight with primary antibodies. The primary antibodies used in the study included rabbit anti-CD45, rabbit anti-MPO, rabbit anti-IL-6, rabbit anti-IL1-β (1:100, Wanleibio Co., Ltd, Wuhan, China), and rabbit anti-TNF-α (1:100, Abclonal, Wuhan, China). The secondary antibody used was an HRP-conjugated donkey anti-rabbit antibody (1:100, Abclonal, Wuhan, China). Signals were visualized with DAB and examined under an Olympus BX53F microscope (Tokyo, Japan). Marker-positive areas in the treatment groups were quantified with ImageJ (National Institutes of Health, USA) relative to those in the control SAL group.

RNA-seq: RNA-seq was performed on spinal cords from SAL, CFA, and DEX-EA groups (*n*=4/group). Total RNA from tissue samples was extracted by QIAGEN RNeasy method, and Nanodrop2000 was used to detect the concentration and purity of the extracted RNA (Masago *et al.,* 2021). Agarose gel electrophoresis was applied to detect RNA integrity, and Agilent5300 was used to determine RQN value. The total amount of RNA required for a single library construction was 1μg, the concentration ≥30ng/μL, RQN >6.5, and OD260/280 between 1.8 and 2.2. PolyA mRNA was enriched with oligo (dT) beads, fragmented (~300bp), and reverse-transcribed to cDNA. After end repair, A-tailing, adapter ligation, and PCR, libraries were quantified by Qubit 4.0 and sequenced on an Illumina NovaSeq X Plus (Majorbio®, Shanghai, China). The RNA-seq datasets underwent processing via RSEM with TPM normalization and DEGs determination through DESeq2 analysis (criteria: $|\log_2 FC| \geq 1$, Padjust <0.05). Hypergeometric distribution was used in enrichment analyses such as Gene Ontology (GO) and Reactome analysis which identified significantly enriched functions in gene sets. The Benjamini-Hochberg (BH) correction method on P-values was used to make corrections on default. The corrected P-value (padjust) which was less than 0.05 was regarded as significantly enriched.

Statistical analysis: Results have been expressed as mean±SD. Inter-group analyses were performed through one-way ANOVA, followed by Tukey's post-hoc testing. Verification of normal distribution of data was carried out by Kolmogorov–Smirnov testing; relationships between cortisol concentrations and nociceptive thresholds underwent evaluation through Pearson's correlation coefficient. The statistical significance threshold was established at P<0.05.

RESULTS

Mechanical pain sensitivity: In this study, a significant increase (P<0.05) in PWT was recorded in the DEX-EA and ST treatments relative to the CFA controls at the second, third and fourth treatment sessions. Inter-treatment group comparison revealed non-significant differences between the DEX-EA and ST treatments. Nevertheless, the DEX-EA therapy demonstrated significantly elevated (P<0.05) PWT measurements relative to both DEX and EA monotherapies at all four treatment sessions (Fig. 1C).

Thermal pain sensitivity: Compared to the CFA controls, the DEX-EA treatment demonstrated significant reductions (P<0.05) in PWL at the first, second, third and fourth treatment sessions. Non-significant PWL variations emerged between the DEX-EA and ST therapies. However, significant PWL increases (P<0.05) were documented in the DEX-EA therapy compared to both DEX and EA monotherapies following the second, third, and fourth treatment sessions (Fig. 1D**)**.

Serum cortisol levels and their correlation with pain sensitivities: The CFA controls displayed a significant increase in serum cortisol concentrations relative to the SAL controls (P<0.01). In contrast, cortisol concentrations were significantly decreased in the ST, EA and DEX-EA treatments compared to the CFA controls (P<0.05). Furthermore, cortisol concentrations significantly decreased (P<0.05) in the DEX-EA therapy relative to the DEX monotherapy (Fig. 1E). It is worth noting that the DEX-EA combination therapy was superior to the two monotherapy treatments, which was demonstrated by stronger and highly significant negative correlation between serum cortisol levels and the nociceptive thresholds (Table 1). These results validate the ability of DEX-EA combination therapy to generate a more stable and potent analgesic effect compared to a monotherapy regimen.

Table 1: Pearson correlation analysis between serum cortisol concentrations and nociceptive mechanical and thermal thresholds in the CFA control, ST, EA, DEX, and DEX-EA groups.

Group	Threshold Type	Correlation (r)	P-value
CFA control	Mechanical	-0.9704	0.0013
	Thermal	-0.9562	0.0028
ST therapy	Mechanical	-0.9349	0.0062
	Thermal	-0.9872	0.0002
DEX monotherapy	Mechanical	-0.9802	0.0006
	Thermal	-0.8849	0.0191
EA monotherapy	Mechanical	-0.9393	0.0054
	Thermal	-0.8616	0.0274
DEX–EA therapy	Mechanical	-0.9722	0.0012
	Thermal	-0.9590	0.0025

Gross evaluation of paw inflammation: A significant increase in inflammatory swelling was recorded in paws of mice from the CFA controls and DEX monotherapy compared to SAL controls (P<0.05) (Fig. 2A). Treatment interventions resulted in decreased inflammatory responses. Particularly, a significant reduction (P<0.05) in paw dimensions of mice was recorded in the DEX-EA treatment compared to the CFA controls (Fig. 2B).

Microscopic evaluation of paw inflammation: The progression of inflammation and the cellular infiltration of inflammatory cells across treatment protocols have been shown in Fig. 3A. There was a significant increase in the inflammatory scores in the CFA controls, ST, DEX, and EA therapies compared to the SAL group (P<0.05). However, non-significant differences were recorded in the combined therapy of DEX-EA compared to the SAL group. Treatment interventions attenuated inflammatory responses, with the ST and DEX-EA therapies achieving significant inflammation score reductions compared to the CFA controls (P<0.05). Additionally, the DEX-EA therapy showed significant decreases in inflammation scoring compared to the DEX monotherapy (Fig. 3B). Proportional inflammatory cell count was significantly increased in the CFA controls, ST, and DEX therapies compared to the SAL group (P<0.005). A significant decrease in the relative cell count was

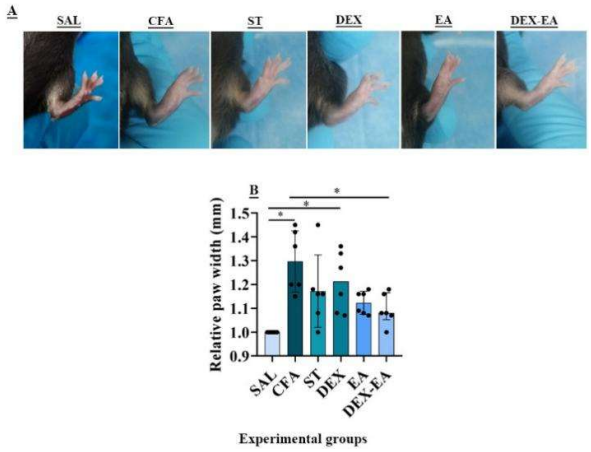

Fig. 2: Paw swelling and thickness (A) and relative paw width (B) comparison between the experimental groups: Saline control (SAL), Complete Freunds Adjuvant (CFA), Standard (ST), Dexmedetomidine (DEX), Electroacupuncture (EA) and Dexmedetomidine-Electroacupuncture (DEX-EA). (*) indicates statistically significant differences (P<0.05).

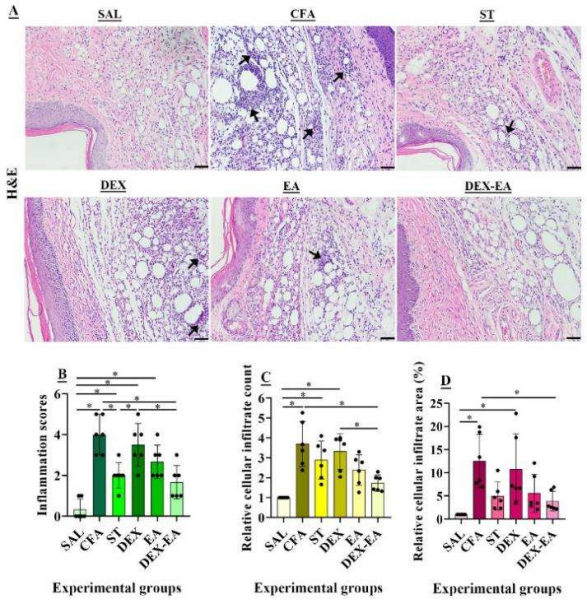

Fig. 3: Inflammation progression and inflammatory cellular infiltration (black arrows) across treatment cohorts (A). Histograms showed inflammatory scores (B), relative cellular infiltrate count (C), and relative cellular infiltrate area (%) (D). Scale bar represents 100μm. (*) denotes statistically significant differences (P<0.05).

observed in the DEX-EA therapy compared to the CFA controls and DEX monotherapy (Fig. 3C). The proportional inflammatory cell area was significantly increased in the CFA controls and DEX monotherapy compared to the SAL group (P<0.05). Moreover, a significant decrease in the relative cell area was noted in the combined therapy of DEX-EA compared to the CFA controls (P<0.05; Fig. 3D).

Immunohistochemical detection of cellular infiltration markers in paw tissue: Representative immunohistochemical images exhibited the expression level of CD45 (Fig. 4A) and MPO (Fig. 4B) in the treatment cohorts. The CD45 immunoreactivity demonstrated significant decrease in the ST, DEX, EA, and DEX-EA treatments relative to the CFA controls (P<0.05). Within treatment groups, the DEX-EA therapy exhibited minimal CD45-positive regions, showing significant reduction compared to the DEX monotherapy (Fig. 4C). Correspondingly, MPO immunoreactivity was significantly decreased in the ST, DEX, EA, and DEX-EA treatments relative to the CFA controls (P<0.05). The DEX-EA therapy also displayed significant MPO-positive area decrease (P<0.05) compared to both ST and DEX treatments (Fig. 4D).

Immunohistochemical detection of inflammatory cytokines in paw tissue: The level of expression of TNF-a, IL-6 and IL-1b was shown using representative immunohistochemical images (Fig. 5A, Fig. 5B and Fig. 5C, respectively). The CFA controls demonstrated higher immunoreactivity for TNF-α compared to the ST, DEX monotherapy, and DEX-EA combination therapy (P<0.05). The expression of TNF-α was the lowest in the combination therapy, and a significant decrease (P<0.05) was observed in the DEX-EA therapy compared to the DEX monotherapy (Fig. 5D). The CFA controls showed a significant increase in the expression level of IL-6 compared to the ST and DEX-EA therapy (P<0.05). The DEX-EA therapy exhibited a significant decrease in the IL-6 expression (P<0.05) compared to DEX and EA monotherapies (Fig. 5E). The expression level of IL-1β was significantly higher in the CFA controls compared to the ST, DEX monotherapy, EA monotherapy, and DEX-EA therapy (P<0.05). The DEX-EA therapy showed significantly lower IL-1β expression compared to the ST and DEX monotherapy (Fig. 5F).

Crosstalk alterations in the spinal cord with DEX-EA treatment in CFA-induced mice: RNA-seq analysis showed distinctive gene expression patterns in the SAL, CFA, and DEX-EA groups: 118 genes (0.75%) in the SAL group, 180 genes (1.14%) in the CFA group, and 254 genes (1.61%) in the DEX-EA group (Fig. 6A). The volcano plot showed a clear separation of differentially expressed genes (DEGs), passing the significance and fold change threshold (Log2FC and an FDR-adjusted P-value <0.05) (Fig. 6B). There were 65 DEGs between the CFA and DEX-EA groups, with 18 genes significantly upregulated and 47 genes downregulated (Fig. 6C). Expression magnitudes of gamma-aminobutyric acid (GABA) A receptor beta 2 subunit (Gabrb2; Fig. $6D_1$), nicotinamide nucleotide transhydrogenase (Nnt; Fig. $6D_2$), guanylate binding protein 6 (Gbp6; Fig. $6D_3$), and c-Maf inducing protein (Cmip; Fig. $6D_5$) demonstrated were significantly increased in the DEX-EA therapy compared to the CFA controls (P<0.05). However, chemokine (C-C motif) ligand 19 (Ccl19; Fig. $6D_4$) was significantly decreased compared to the CFA controls (P<0.05). Additionally, the CFA controls exhibited a significant decrease in the Gabrb2 (P<0.05) and an increase in the Ccl19 (P<0.05) compared to the SAL group.

The heat map illustrates the differential expression of genes in each spinal cord sample across the SAL, CFA, and DEX-EA groups (Fig. 7A). Inspiring patterns emerged in the GO analysis between the CFA and DEX-EA groups. Our findings revealed enriched processes related to

catabolic pathways, including cellular catabolic processes, nuclear transcribed mRNA catabolic processes, processes utilizing autophagic mechanisms, and cellular nitrogen compound catabolic processes (Fig. 7B). In addition, Reactome revealed that there was an enrichment of metabolic processes related to cell energy production and expenditure, pyruvate metabolism, citric acid (TCA) cycle, and respiratory electron transport (Fig. 7C). Statistical assessment via one-way ANOVA identified significant variations in mitochondrial gene expression between the CFA and DEX-EA cohorts, specifically involving mitochondrially encoded ATP synthase 6 (mt-Atp6), mitochondrially encoded 16S rRNA (mt-Rnr2), mitochondrially encoded NADH dehydrogenase 3 (mt-Nd3), and mitochondrially encoded cytochrome c oxidase I (mt-Co1; Fig. 7D).

DISCUSSION

The present study examined the impact of acupoint-injected DEX and EA in the reduction of inflammatory pain in the CFA model. The DEX-EA treatment exhibited a high level of pain thresholds as compared to both DEX and EA monotherapies. This demonstrates the possibilities of synergism in using DEX and EA to counter inflammatory pains. Our findings concur with earlier studies that indicated the efficacy of multimodal therapies over single treatment strategies for pain management (Creighton et al., 2019; Shi and Wu, 2023). A negative relationship was also found for blood cortisol and pain threshold. This seems to be due to the consequence of the stress response to inflammation and tissue injury. A study on chronic inflammatory pain in rats also showed high concentrations of circulating corticosterone, with associations between anxiety-like behavior and changes in DNA methylation in the amygdala (spinieli *et al*., 2022). The current study indicated that the CFA without treatment intervention had significantly higher paw inflammatory changes compared to the treatment groups. It has also been demonstrated that CFA administration leads to inflammation and migration of macrophages, in addition to the production of pro-inflammatory cytokines, such as TNF- a, IL-6 and IL-1b (Lazarević *et al*., 2024). Animals receiving DEX-EA therapy had better mitigations in the form of inflammation scoring, and the extent of inflammatory cell accumulation, than to DEX alone. These results indicate the possible synergistic effect of DEX and EA, which causes greater therapeutic effects. This novel treatment regime can suppress inflammation and subsequently pain by suppressing inflammation signaling pathways.

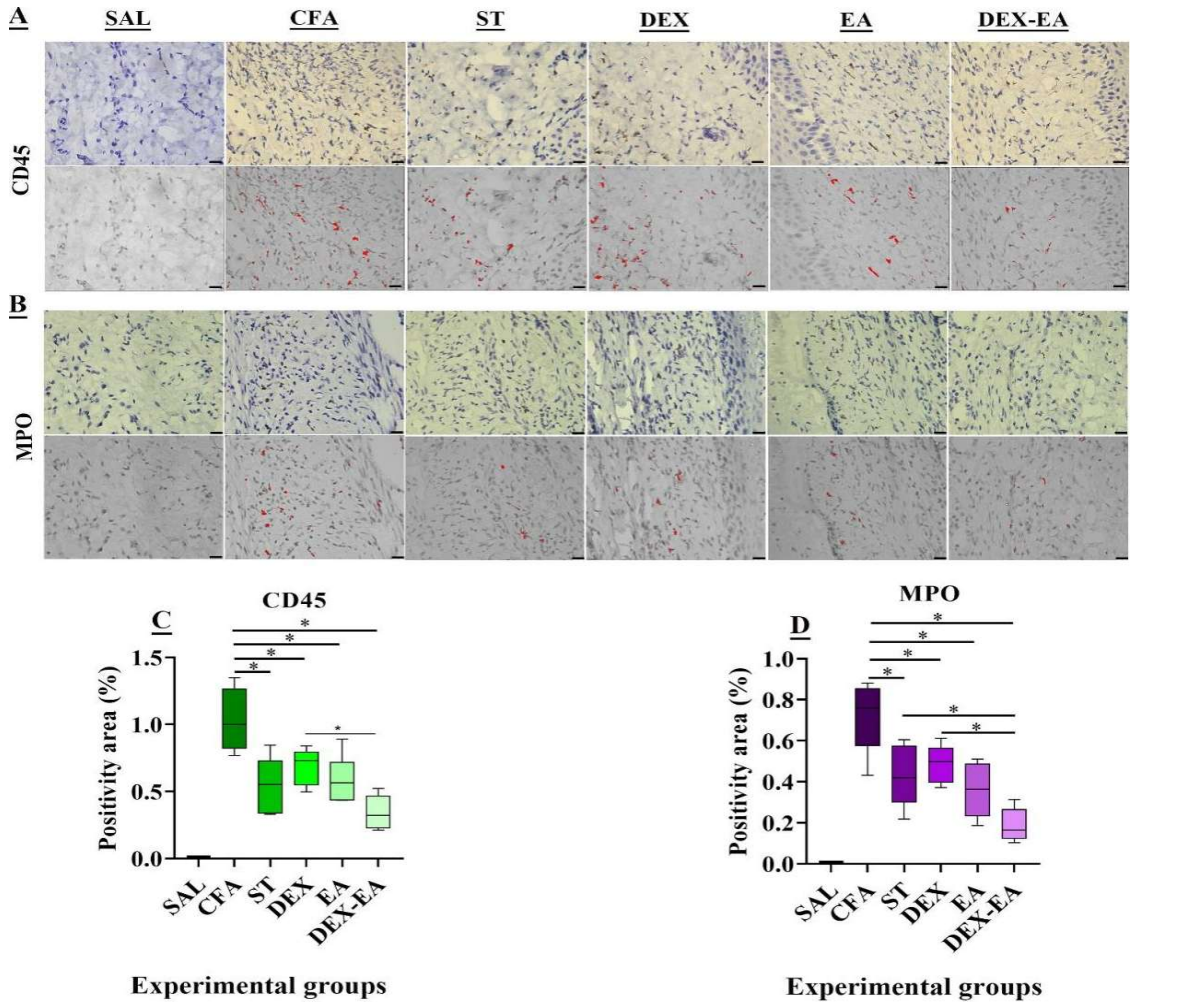

Fig. 4: Immunoreactivity of CD45 (A) and myeloperoxidase (MPO) (B) within paw tissue specimens across experimental cohorts. Histograms showed the positivity area of CD45 (C) and MPO (D). Scale bar indicates 20μm. (*) shows statistically significant differences (P<0.05).

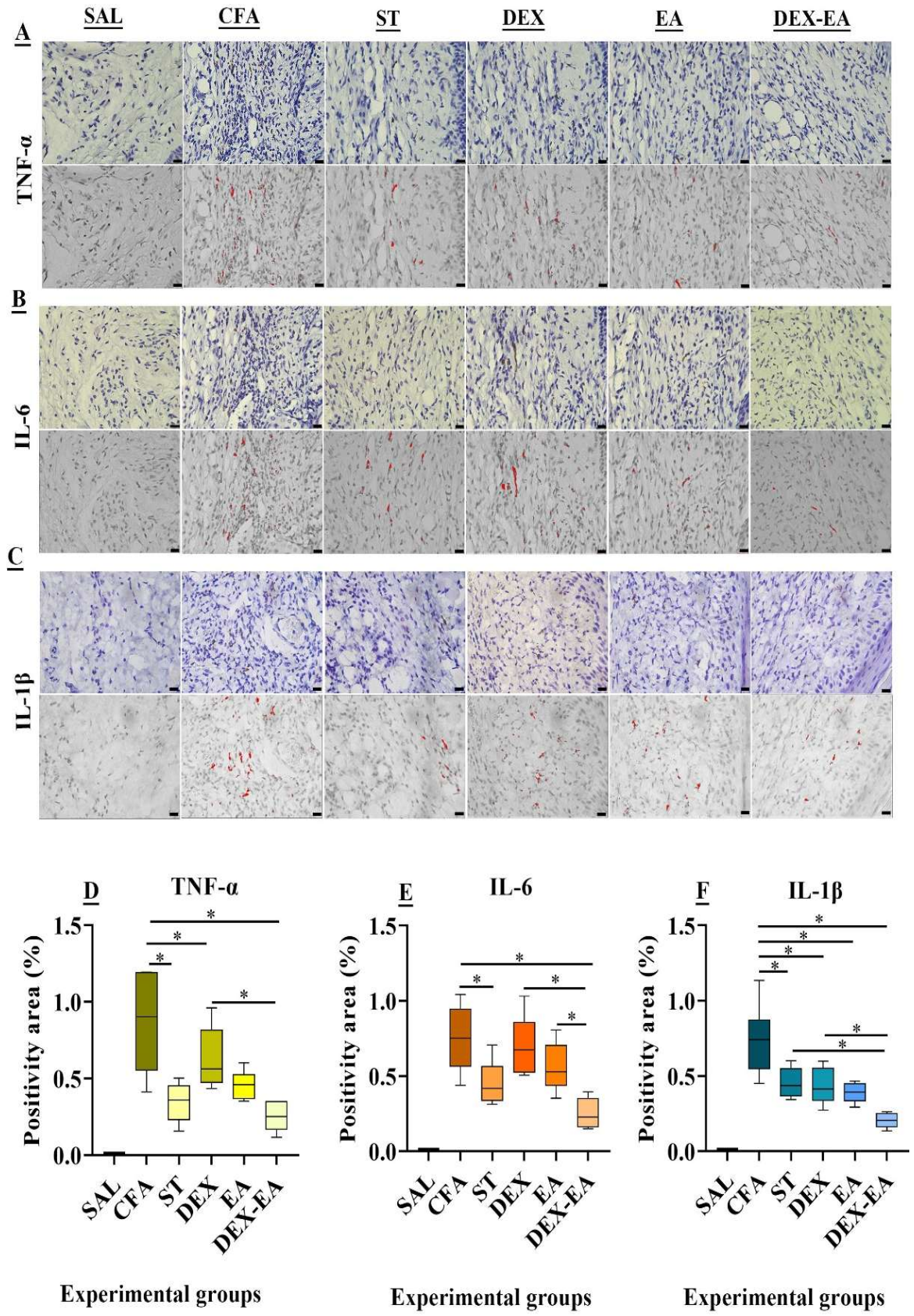

Fig. 5: Immunoreactivity of tumor necrosis factor-alpha (TNF-α) (A), interleukin-6 (IL-6) (B), and interleukin-1 beta (IL-1β) (C) within paw tissue specimens across treatment cohorts. Histograms show the positivity area of TNF-α (D), IL-6 (E), and IL-1β (F). Scale bar represents 20μm. (*) denotes statistically significant differences (P<0.05).

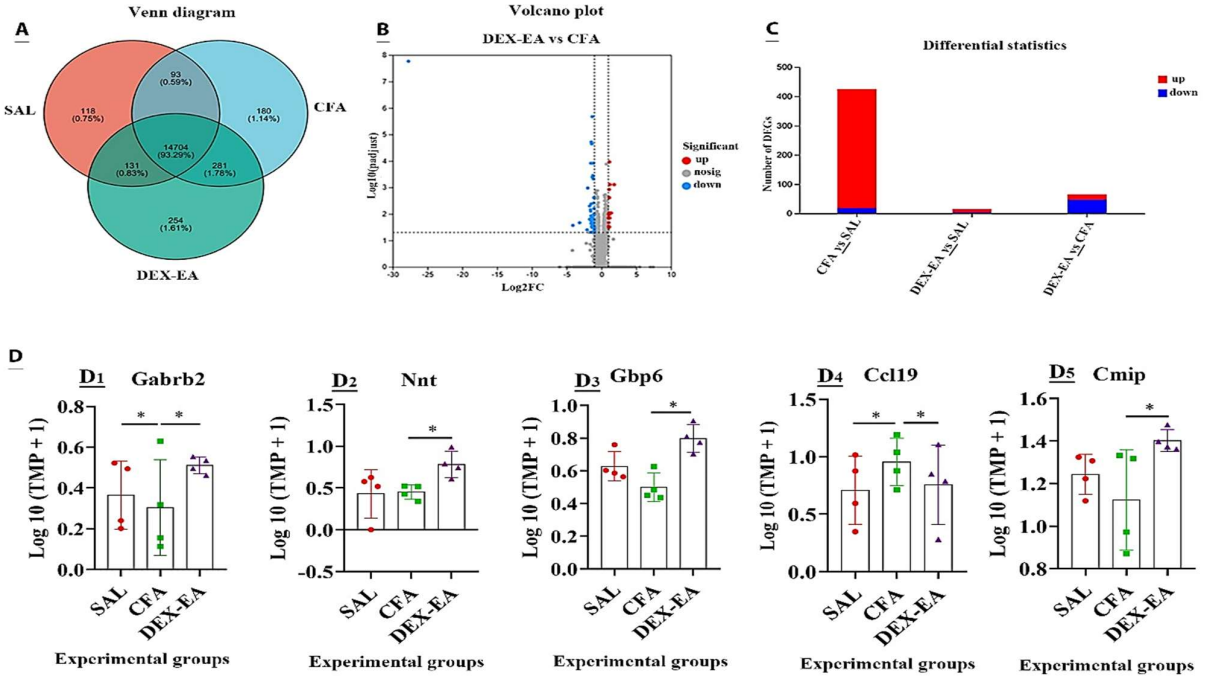

Fig. 6: A): Venn representation illustrating quantity and proportion of distinct and overlapping gene expression patterns within spinal cord tissue across saline control (SAL), Complete Freund's Adjuvant treatment (CFA), and combination DEX-EA therapy. B): Volcano plot visualization depicting significantly upregulated (red markers) and downregulated (blue markers) genes between the CFA and combined DEX-EA cohorts. C): Display of differentially expressed genes (DEGs) identified through inter-group comparisons: CFA versus SAL, DEX-EA versus SAL, and DEX-EA versus CFA. D): Comparative evaluation of log10-transformed transcript abundance (TPM+1) for Gabrb2 (D_1), Nnt (D_2), Gbp6 (D_3), Ccl19 (D_4), and Cmip (D_5). Log10 transcript abundance values expressed as mean±SD. Asterisks (*) signify statistically significant differences ($P<0.05$).

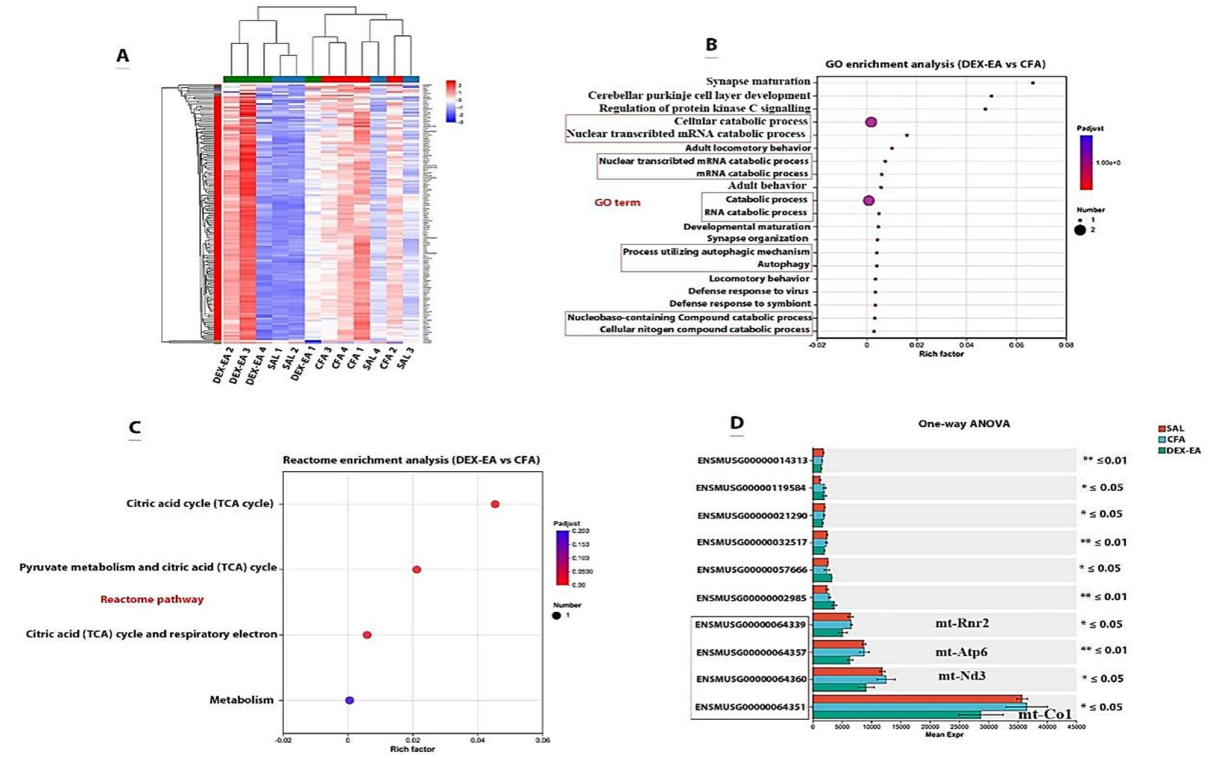

Fig. 7: A): Visualization of a heat map illustrating the profile of gene expression of the spinal cord in the samples of treatment groups. The columns are individual samples and the rows to certain genes. The intensity of expression is represented by color gradients where red implies high expression and blue implies low expression. B): Gene Ontology (GO) enrichment analysis between DEX-EA and CFA cohorts. The vertical dimension represents GO terminology with a focus on catabolic process pathways and the horizontal dimension reflects the values of Rich factors. C): Findings on reactome pathway enrichment between DEX-EA and CFA treatment groups. Vertical orientation depicts Reactome pathway designations whereas horizontal orientation represents Rich factor measures. D): Statistical testing on the basis of one-way ANOVA revealed significant differences in the expression between the treatment groups. Y-axis shows the gene identifiers of the mitochondrial genes (mt-Rnr2, mitochondrial-Atp6, mitochondrial-Nd3 and mitochondrial-Co1) and the X-axis shows the relative magnitudes of gene expression.

According to the past reports, DEX can suppress inflammation through the inhibition of NF-KB signaling and the release of attenuated cytokines (Li *et al.,* 2015; Ji *et al.,* 2017). Also, EA could possess anti-inflammatory properties due to its ability to regulate vagal activity and promote endogenous opioid secretion (Wang and Liu, 2021; Yang *et al.,* 2024). Past research that employed chronic models of inflammation and arthritis revealed that EA reduced inflammatory response by regulating the synthesis of proinflammatory cytokines (Gondim *et al.,* 2012; Lan *et al.,* 2024). The CD45 immunoreactivity in paw tissue was much lower in the DEX-EA therapy as compared to the DEX monotherapy. Likewise, MPO immunoreactivity was significantly reduced in the DEX-EA group compared to the DEX group. In the published literature, DEX has also been shown to decrease oxidative stress and inflammation by decreasing leukocyte recruitment and modulating the expression of adhesion molecules in inflammatory cells. Therefore, it appears that the DEX+EA could both effectively decrease inflammatory responses through the reduction of inflammatory cell infiltration and neutrophil recruitment into the paw (Wang *et al.,* 2019; Wang and Liu, 2021). Most importantly, DEX could reduce oxidative stress and the acute inflammatory process by interfering with the activation of neutrophils and the synthesis of MPO (Yao *et al.,* 2023). Electroacupuncture could suppress neutrophil-driven inflammation as a result of increased hyperemia with modulation of local tissue anti-inflammatory responses (Park and Namgung, 2018; Lan *et al.,* 2024). In earlier studies, it has been shown that the CFA induces substantial increases in inflammatory cytokines (Weng *et al.*, 2021; Lazarević *et al.*, 2024), which cause tissue damage with paw tissue damage and inflammation cell infiltration. The DEX-EA treatment showed reduced cytokines than the DEX treatment which showed reduced paw inflammation. Yamazaki *et al.* (2022) and Li *et al.* (2023) claim that DEX therapy leads to cytokine reduction through the regulation of the sympathetic nervous system activation, thus avoiding stress responses. Electroacupuncture suppresses the inflammatory process and favors the healing of inflammation (Wang *et al.,* 2009). The current study incorporated the analgesic and anti-inflammatory properties of diclofenac sodium (DS) as a conventional management of CFA-induced paw inflammation. The combination of DEX-EA regimen and DS was discovered to be much more effective in enhancing the pain thresholds and in alleviating the paw inflammation. This implies that DEX-EA has the same effect as that of DS. These findings are consistent with the previous reports that used DS in inflammatory models as a positive control drug (Dina *et al.,* 2010; Gupta *et al.,* 2015). Collectively, DEX-EA could be a great relief of inflammatory pain and could contribute to the reduction of adverse effects caused by traditional therapies by reducing the dose of anti-inflammatory medications needed.

The RNA-seq analysis in this research detected an interesting discrepancy in the expression of the genes in the spinal cord of CFA control and DEX-EA groups. These results may give a potential reason why the DEX and EA were synergistic when it comes to alleviating pain in the case of inflammation. The pain (Gabrb2: GABA A receptor subunit beta 2), immune (Ccl19: chemokine ligand 19), and inflammatory (Cmip: c-Maf inducing protein) modulations through the involvement of the DEGs have been adopted to reduce pain and inflammation. The GO analysis revealed that there were important enriched pathways of autophagic and catabolic processes in the DEX-EX treatment in contrast to the CFA model. Gene regulation of autophagic pathways is also necessary in reducing the inflammatory response and reducing tissue damage (Yao *et al.,* 2021; Stifel *et al.,* 2022). It has recently been shown that DEX is capable of causing autophagic influx and subsequently lessening inflammatory damage (Yang *et al.,* 2020; Xu *et al.,* 2022).

The dysfunction of mitochondria is a critical part of the development of pain and other inflammatory diseases (Doyle and Salvemini, 2021). On the contrary, the central improvement of mitochondrial work and the increase in energy production leads to inflammation reduction (Missiroli *et al.,* 2020; Marchi *et al.,* 2023). In the DEX-EA regimen, there were significant changes in the expression of mitochondrial genes. Furthermore, the Reactome analysis revealed enriched metabolic pathways related to the mitochondrial energy production in the DEX-EA treatment in comparison with the CFA model. Recent studies have proved that the alteration in the mitochondrial activity can affect the inflammatory processes and nociceptive inputs. Mitochondrial dysfunction may be a result of chronic inflammation, and this dysfunction will lead to a reduction in the generation of energy in the cells and the continuation of the pain signal (Ribeiro *et al.,* 2022; Yang *et al.,* 2023). The DEX-EA treatment that was performed showed a significant reduction in genes associated with immunological reactions, including Ccl19, which is a key factor in inflammation and pain (Park and Namgung, 2018; Lan *et al.,* 2024). These findings support the role of the DEX-EA therapy in the process of inflammation, and possibly by reducing the recruitment of inflammatory cells in the injury sites.

Conclusions: There could be a synergistic effect between acupoint-administered DEX and EA in the alleviation of inflammation and pain. We propose that the treatment of DEX-EA can regulate the genes associated with the immune cell response and the neurotransmission of pain. As a result, using DEX acupoint injections in conjunction with EA may offer a novel approach to managing inflammatory pain.

Authors contribution: Conceptualization and experimental design were carried out by MMA, ES and YD. Methodology was performed by MMA and ES, while data curation was handled by MMA and ES. Validation was conducted by MMA, HL, ES and AR, and visualization was completed by MMA, ES, ML, AR and MKM. Software tasks were performed by MMA, ES and HF, while formal analysis was done by MMA, and ES. Investigation was conducted by MMA, ES, FAK, YD and MD. Funding acquisition and resources were the responsibility of YD and HF. The original draft was written by MMA and ES, and the review and editing were completed by MMA, HL, ES, ML, AR, MKM, FAK, YD, MD and HF. Project administration was managed by MMA, ES, HF and YD, while supervision was provided by

MMA, YD and MD. All authors have read and approved the final version of the manuscript.

Acknowledgements: This work was partially supported by Hubei Province Experimental Animal Science and Technology Program Project (2024CFC004) and National Key R&D Program of China (Grant No: 2023YFD1801104-6).

Data availability statement: The original data presented in the study are openly available at FigShare repository at https://doi.org/10.6084/m9.figshare.28787744

Ethics approval and consent to participate: All experimental procedures adhered to the ethical guidelines of Animal Experimental Ethical Inspection of Laboratory Animal Center, Huazhong Agricultural University (No: HZAUMO-2025-0141).

Competing interests: The authors declare no conflict of interest.

REFERENCES

Cao DL, Zhang ZJ, Xie RG, *et al.*, 2014. Chemokine CXCL1 enhances inflammatory pain and increases NMDA receptor activity and COX-2 expression in spinal cord neurons via activation of CXCR2. Experimental Neurology 261: 328-36.

Creighton DW, Kumar AH and Grant SA, 2019. Perioperative multimodal pain management: an evidence-based update. Current Anesthesiology Reports 9:295–307.

Dina TA, Taslima MA, Ahmed NU, *et al.*, 2010. Analgesic and anti-inflammatory properties of *Argyreia argentea* methanol extract in animal model. Journal of Taibah Univeristy for Science 3(1): 1-7.

Doyle TM and Salvemini D, 2021. Mini-Review: Mitochondrial dysfunction and chemotherapy-induced neuropathic pain. Neuroscience Letters 760:136087.

Gondim DV, Costa JL, Rocha SS, *et al.*, 2012. Antinociceptive and anti-inflammatory effects of electroacupuncture on experimental arthritis of the rat temporomandibular joint. Canadian Journal of Physiology and Pharmacology 90:395–405.

Gupta AK, Parasar D, Sagar A, *et al.,* 2015. Analgesic and anti-inflammatory properties of gelsolin in acetic acid induced writhing, tail immersion and carrageenan induced paw edema in mice. PloS One 10(8): e0135558

Ho KY, Gwee KA, Cheng YK, *et al.*, 2018. Nonsteroidal anti-inflammatory drugs in chronic pain: implications of new data for clinical practice. Journal of Pain Research 11:1937–48.

Hussein SZ, Yusoff KM, Makpol S, *et al.*, 2013. Gelam honey attenuates carrageenan-induced rat paw inflammation via NF-κB pathway. PLoS One 8:e72365.

Ji D, Zhou Y, Li S, *et al.,* 2017. Anti-nociceptive effect of dexmedetomidine in a rat model of monoarthritis via suppression of the TLR4/NF-κB p65 pathway. Experimental and Therapeutic Medicine 14(5):4910–18.

Koo ST, Kim SK, Kim EH, *et al.* 2010. Acupuncture point locations for experimental animal studies in rats and mice. Korean Journal of Acupuncture 27(3):67–78.

Lan Y, Jing X, Zhou Z, *et al.*, 2024. Electroupuncture ameliorates inflammatory pain through CB2 receptor-dependent activation of the AMPK signaling pathway. Chinese Medicine 19(1):176.

Lazarević M, Stanisavljević S, Nikolovski N, *et al.*, 2024. Complete Freund's adjuvant as a confounding factor in multiple sclerosis research. Frontiers in Immunology 15:1353865.

Li B, Li Y, Tian S, *et al.,* 2015. Anti-inflammatory effects of perioperative dexmedetomidine administered as an adjunct to general anesthesia: A meta-analysis. Scientific Reports 5(1):12342.

Li J, Zhang H, Deng B, *et al.*, 2023. Dexmedetomidine improves anxiety-like behaviors in sleep-deprived mice by inhibiting the p38/MSK1/NFκB pathway and reducing inflammation and oxidative stress. Brain Sciences 13:1058.

Li S, Xie P, Liang Z, *et al.*, 2018. Efficacy comparison of five different acupuncture methods on pain, stiffness, and function in osteoarthritis of the knee: A network meta-analysis. Evidence Based Complementary and Alternative Medicine 2018:1638904.

Liu L, Abouelfetouh MM, Ding, Y, *et al.*, 2025. Electroacupuncture combined with subanesthetic alfaxalone as a novel target for alleviating neuropathic pain. Pain Reports 10(5): e1296

Lynch ME and Watson CPN, 2006. The pharmacotherapy of chronic pain: A review. Pain Research & Management 11(1):11–38.

Manglik A, Lin H, Aryal DK, *et al.*, 2016. Structure-based discovery of opioid analgesics with reduced side effects. Nature 537:185–90.

Marchi S, Guilbaud E, Tait S, *et al.,* 2023. Mitochondrial control of inflammation. Nature Reviews Immunology 23(3):159-73

Masago K, Fujita S, Oya Y, *et al.,* 2021. Comparison between fluorimetry (Qubit) and spectrophotometry (NanoDrop) in the quantification of DNA and RNA extracted from frozen and FFPE tissues from lung cancer patients: A real-world use of genomic tests. Medicina 57(12), 1375.

Missiroli S, Genovese I, Perrone M, *et al.,* 2020. The role of mitochondria in inflammation: From cancer to neurodegenerative disorders. Journal of Clinical Medicine 9(3): 740.

Oikonomou P, Nikolaou C, Papachristou F, *et al.,* 2023. Eugenol reduced MPO, CD45 and HMGB1 expression and attenuated the expression of leukocyte infiltration markers in the intestinal tissue in biliopancreatic duct ligation-induced pancreatitis in rats. Medicina 60(1):74.

Park JY and Namgung UK, 2018. Electroacupuncture therapy in inflammation regulation: current perspectives. Journal of Inflammation Research 11: 227–37.

Park KS, Kim C, Kim JW, *et al.*, 2023. a pragmatic randomized controlled trial on the effectiveness and safety of pharmacopuncture for chronic lower back pain. Journal of Pain Research 16:2697–2712.

Ribeiro PSS, Willemen HLDM and Eijkelkamp N, 2022. Mitochondria and sensory processing in inflammatory and neuropathic pain. Frontiers in Pain Research 3:1013577.

Shi Y and Wu W, 2023. Multimodal non-invasive non-pharmacological therapies for chronic pain: mechanisms and progress. BMC Medicine 21:372.

Son JY, Goo K, Kim NY, *et al.*, 2024. Effectiveness and safety of pharmacopuncture on inpatients with tension headache caused by traffic accidents: a pragmatic randomized controlled trial. Journal of Clinical Medicine 13:4457.

Spinieli RL, Cazuza RA, Sales AJ, *et al.*, 2022. Persistent inflammatory pain is linked with anxiety-like behaviors, increased blood corticosterone, and reduced global DNA methylation in the rat amygdala. Molecular Pain 18:17448069221121307.

Stifel U, Caratti G and Tuckermann J, 2022. Novel insights into the regulation of cellular catabolic metabolism in macrophages through nuclear receptors. FEBS Letters 596:2617–2629.

Suvarna S, Layton C, and Bancroft J, 2013. The hematoxylins and eosin. Bancroft's Theory and Practice of Histological Techniques, 7th Ed; Churchill Livingstone, London, UK, pp:172-186.

Vieira JS, Toreti JA, de Carvalho RC, *et al.*, 2018. Analgesic effects elicited by neuroactive mediators injected into the ST 36 acupuncture point on inflammatory and neuropathic pain in mice. Journal of Acupuncture and Meridian Studies 11:280–89.

Wan J, Nan S, Liu J, *et al.,* 2020. Synaptotagmin 1 is involved in neuropathic pain and electroacupuncture-mediated analgesic effect. International Journal of Molecular Sciences 21(3):968.

Wang K, Wu M, Xu J, *et al.,* 2019. Effects of dexmedetomidine on perioperative stress, inflammation, and immune function: systematic review and meta-analysis. British Journal of Anaesthesia 123(6): 777-94.

Wang X and Liu Q, 2021. Dexmedetomidine relieved neuropathic pain and inflammation response induced by CCI through HMGB1/TLR4/NF-κB signal pathway. Biological and Pharmaceutical Bulletin: doi: 10.1248/bpb.b21-00329 (online ahead of print).

Wang J, Zhao H, Mao-Ying QL, *et al.*, 2009. Electroacupuncture downregulates TLR2/4 and pro-inflammatory cytokine expression after surgical trauma stress without adrenal glands involvement. Brain Research Bulletin 80:89–94.

Weng W, Wang F, He X, *et al.*, 2021. Protective effect of corynoline on the CFA induced rheumatoid arthritis via attenuation of oxidative and inflammatory mediators. Molecular and Cellular Biochemistry 476:831–39.

Xu Q, Niu C, Li J, *et al.*, 2022. Electroacupuncture alleviates neuropathic pain caused by spared nerve injury by promoting AMPK/mTOR-

mediated autophagy in dorsal root ganglion macrophage. Annals of Translation Medicine 10(24): 1341.

Yamazaki S, Yamaguchi K, Someya A, *et al*., 2022. Anti-inflammatory action of dexmedetomidine on human microglial cells. International Journal of Molecular Sciences 23:10096.

Yang H, Wang Y, Zhen S, *et al*., 2023. AMPK activation attenuates cancer-induced bone pain by reducing mitochondrial dysfunction-mediated neuroinflammation: AMPK activation attenuates bone cancer pain. Acta Biochimica Biophysica Sinica (Shanghai) 55:460.

Yang H, Zhao Y, Chen Y, *et al*., 2024. dexmedetomidine alleviates acute stress-induced acute kidney injury by attenuating inflammation and oxidative stress via inhibiting the P2X7R/NF-κB/NLRP3 pathway in rats. Inflammation 48(1):412-25.

Yang T, Feng X, Zhao Y, *et al*., 2020. Dexmedetomidine enhances autophagy via α2-AR/AMPK/mTOR pathway to inhibit the activation of NLRP3 inflammasome and subsequently alleviates lipopolysaccharide-induced acute kidney injury. Frontiers in Pharmacology 11:790.

Yao J, Lan B, Ma C, *et al*., 2023. RNA-sequencing approach for exploring the protective mechanisms of dexmedetomidine on pancreatic injury in severe acute pancreatitis. Frontiers in Pharmacology 14:1189486.

Yao RQ, Ren C, Xia Z-F, *et al*., 2021. Organelle-specific autophagy in inflammatory diseases: a potential therapeutic target underlying the quality control of multiple organelles. Autophagy 17:385–401.

Yu MI, Wei Rd, Zhang T, *et al*., 2021. Electroacupuncture relieves pain and attenuates inflammation progression through inducing IL-10 production in CFA-induced mice. Inflammation 43:1233–45.